ELSEVIER

Journal of Power Sources 62 (1996) 95–99

JOURNAL OF POWER SOURCES

Partial oxidation of methane in solid oxide fuel cells: an experimental evaluation

V. Antonucci [a], P.L. Antonucci [b], A.S. Aricò [a], N. Giordano [a]

[a] *Institute CNR–TAE, via Salita S. Lucia 39, 98126 S. Lucia, Messina, Italy*

[b] *University of Reggio Calabria, Faculty of Engineering, Institute of Chemistry, via Cuzzocrea 48, 98128 Reggio Calabria, Italy*

Received 23 November 1995; accepted 21 February 1996

Abstract

Operation results of a 150 W tubular solid oxide fuel cell stack prototype, directly fuelled by methane, are presented. Fuel is partially oxidized to synthesis gas as an alternative route to steam reforming. An extensive electrochemical investigation, consisting in the analysis of the performance attained during a 3000 h endurance test, shows the feasibility of the process.

Keywords: Solid oxide fuel cell; Methane partial oxidation; Synthesis gas

1. Introduction

The hydrogen-fuelled solid oxde fuel cell (SOFC) technology has attained, in the last decade, a real maturity testified by the development of stack units of different configurations and sizes. Nevertheless, the direct utilization of natural gas represents one of the key aspects which makes SOFC, amongst the other fuel cell systems, potentially more competitive within the present technologies for energy production.

The most acknowledged process for generation of hydrogen for fuel cells is based upon the steam reforming of methane in internal configuration. However, due to the endothermicity of the reaction, special attention has to be paid to the maintenance of the operational heat balance, in order to avoid other possible problems, in terms of carbon deposition in the fuel electrode. An alternative route to the direct utilization of natural gas in SOFC is represented by the partial oxidation to synthesis gas

$$CH_4 + 1/2O_2 \rightarrow 2H_2 + CO \quad \Delta H^0_{298} = -35.6 \text{ kJ/mol} \quad (1)$$

the reaction being slightly exothermic and more selective to CO, i.e. with a higher CO/H_2 ratio in the reaction products than in the steam reforming.

Some advantages with respect to steam reforming have been claimed in terms of lower fuel specific consumption and higher productivity [1–3]; moreover, due to its oxidative nature, oxyreforming would present, in principle, other positive aspects, as a greater sulfur tolerance and less coking phenomena. The development of a proper catalyst, however, still represents an open question whatever the selected process.

The practical reliability of the process has been tested, on laboratory scale, operating with a 150 W, sixteen-cell tubular stack. The results have allowed to assess the suitability of the system for the direct use of methane/air mixtures, with the achievement of the target power and a long-life expectance. On these established bases, future opportunities of cell scaling-up and components optimization have been identified to go further on the way of cost effective operations.

2. Partial oxidation reaction

Oxyreforming of methane occurs under fuel-rich conditions ($CH_4/O_2 \cong 2$). The reaction involves an instant combustion of a fraction (25%) of the methane fed

$$CH_4 + 2O_2 \rightarrow CO_2 + 2H_2O \quad \Delta H^0_{298} = -886.16 \text{ kJ/mol} \quad (2)$$

with a complete consumption of the stoichiometrically limited oxygen.

The remaining quantity of CH_4 is reformed in both H_2O and CO_2 according to the reactions

$$CH_4 + H_2O \leftrightarrow CO + 3H_2 \quad \Delta H^0_{298} = 226 \text{ kJ/mol} \quad (3)$$

$$CH_4 + CO_2 \leftrightarrow 2CO + 2H_2 \quad \Delta H^0_{298} = 261 \text{ kJ/mol} \quad (4)$$

$$CO + H_2O \leftrightarrow CO_2 + H_2 \quad \Delta H^0_{298} = -41.19 \text{ kJ/mol} \quad (5)$$

PII S0378-7753(96)02411-1

As temperature increased, the endothermic reactions (3) and (4) are favoured, and CO and H_2 become the main reaction products.

Under working conditions, reactions (1)–(4) are generally accompanied by carbon-forming reactions, such as:

$$2CO \rightarrow C + CO_2 \qquad \Delta H^0_{298} = -172.4 \text{ kJ/mole} \qquad (6)$$

$$CH_4 \rightarrow C + 2H_2 \qquad \Delta H^0_{298} = 75.9 \text{ kJ/mol} \qquad (7)$$

$$CO + H_2 \rightarrow C + H_2O \qquad \Delta H^0_{298} = -132 \text{ kJ/mol} \qquad (8)$$

The partial oxidation reaction has been previously investigated on laboratory scale [4–6]; now, integration of this process in SOFC for electrical energy production has been experimentally tested to verify this route as an alternative option to steam reforming.

3. Description of the 150 W stack prototype

The prototype is constituted by 16 tubular monocells electrically connected in series; the co-flow feed of gases results in a compact geometry of the system. The monocell is self-supporting, as the ceramic tube supports the deposited electrode; each tube has a thickness of 0.3 mm and it is closed at its lower edge. Relevant single cell and stack parameters are reported in Table 1.

The electrolyte material is an yttria-scandia stabilized zirconia (YSSZ + ZrO_2 = 90%; Sc_2O_3 = 6%, and Y_2O_3 = 4%). Anode (Pt–Ni–CeO_2/YSSZ) and cathode (Pt–PrO_2) layers are deposited by slurry painting onto the outer and inner part of the ceramic tube, respectively.

Anode feed inlets are located in a lateral position on the lower part of the stack; mixing of the gases occurs in the tube portion immediately preceding the electrochemical section. Cathodic air inlet is located in the middle position of the upper panel of the stack, and successively divided into sixteen paths through a cubic stainless-steel distribution module including sixteen quartz air injectors. Heat resulting by fuel utilization is used to warm up the oxidant entering into the cathode compartment, see Fig. 1.

Table 1
Cell and stack parameters

a) *Single cell*	
Diameter (mm)	10
Length (mm)	210
Wall thickness (mm)	0.3–0.4
Operating area (cm^2)	63
b) *Stack*	
Volume of the electrochemical section (cm^3)	500
Total operating area (cm^2)	1000
Overall dimensions	
Height (mm)	750
Diameter (mm)	250
Weight	
Electrochemical components (kg)	2.0
Auxiliaries (kg)	10

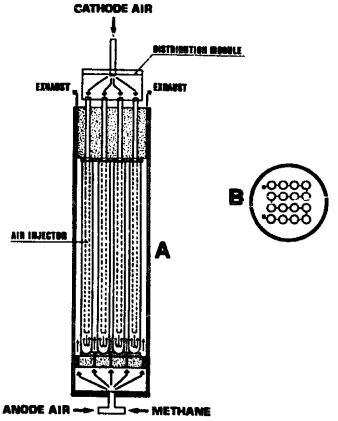

Fig. 1. Schematic view of the fuel cell stack: (A) front, and (B) top.

The upper part of the stack is thermally insulated by a preformed refractory module allowing the allocation of eight thermocouples and *I–V* platinum wires for each monocell.

Monitoring and manipulation of the operational parameters of the stack are achieved by the presence of proper control and regulation devices; a PC-interfaced data logger allows data handling during performance and life-time tests under different operation conditions [7].

4. Results and discussion

Fig. 2 shows a typical *I–V* curve of the stack, obtained under the following conditions: T = 950 °C; O_2/CH_4 = 0.5 (stoichiometric); CH_4: 0.84 l/min; anode air: 2.0 l/min; cathode air: 12.0 l/min. Internal resistance measurements of

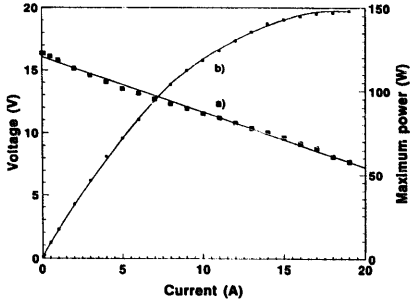

Fig. 2. (a) *I–V* and (b) power characteristics of the 150 W stack prototype.

the stack, carried out with the current interruption method, gave a value of 0.37 Ω.

The *V–I* slope in Fig. 2 is in close agreement with the measured uncompensated resistance; this evidence, together with the linear *V–I* variation, accounts for a typical resistive behaviour in the operating current range of the stack at the selected flow rate of reagents.

To give a better insight into the potentialities of the process under investigation, particular attention has been paid to the influence of the air/CH_4 ratio, at different fuel flow rates, on the cell performance.

Fig. 3 shows the variation of maximum power of the stack obtained by polarization curves; it is observed that the output power decreases with the decrease of gas flow. These results clearly account for a mass-transport controlling process in determining, at low flow rates (curves 2, 3, 4) (together with the uncompensated resistance) the polarization behaviour, resulting in a lower output power. As opposite, curve 1, obtained under excess fuel conditions, denotes a purely resistive behaviour. The observed variation of output power with composition at the same flow rate reflects the variation of e.m.f. values with the O_2/CH_4 ratio (Fig. 4). In fact, the

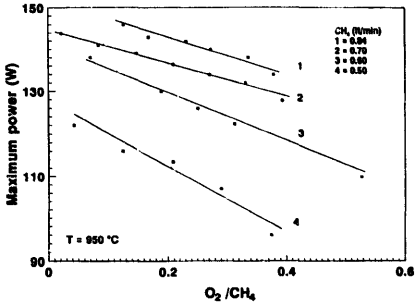

Fig. 3. Influence of the air/methane ratio on the maximum power of the stack.

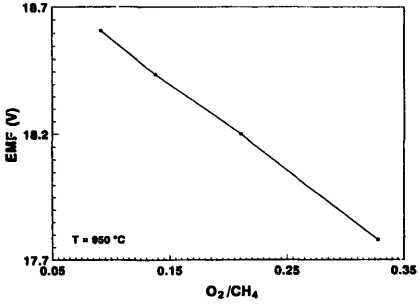

Fig. 4. Influence of the air/methane ratio on the e.m.f. of the stack at 950 °C.

e.m.f. value is strictly related to the partial pressure of reactants fed to anode and cathode. The oxygen partial pressure at the cathode is determined by the oxygen content in air; the presence of some amount of oxygen in the methane stream fed to the anode determines an increase in the reversible potential value with respect to NHE (normal hydrogen electrode) for the anode reaction. This produces a decrease in the e.m.f. values. Moreover, deviations from the reaction stoichiometry, in fact, give rise to parallel reactions, according to the deep CH_4 oxidation in case of presence of excess air (reaction (2)) or reforming by H_2O and/or CO_2 in the reaction mixture (reactions (3) and (4)) in case of substoichiometric oxygen/CH_4 ratios. Besides, carbon deposition is easily attained in the latter situation, i.e. under oxygen-deficient conditions.

These results, although preliminary, make evident that a catalyst based on a ceria-promoted zirconia and a noble metal allows to reach useful electrochemical efficiencies, which survive even when the oxidant to fuel ratio is kept very low. In this respect, it is well known that cerium oxide exhibits appreciable catalytic activity for carbon gasification in air at temperatures in the 500–1000 °C range. The catalytic effect has been attributed to a redox process involving the cyclic conversion of the oxide from the Ce(IV) to the Ce(III) oxidation state [8]. More recently, CeO_2 was found to convert methane into synthesis gas at 873–1073 K; the reaction was accelerated in the presence of 1% Pt black [9].

In consideration of the general behaviour observed in out-of-cell experiments [10], it appears that a localized total combustion of a small fraction of CH_4 (depending upon the selected O_2/CH_4 ratio) occurs at the very extreme edge of the anode, even in presence of low air/CH_4 ratios, enough to sustain averaged isothermal conditions with a sharp T peak at the inlet. According to the reaction path previously depicted, the trend of the temperature of anode gas along the cell (Fig. 5, curve 1) shows a sudden increase in temperature due to the exothermicity of the methane combustion, then the sharp temperature drop is associated with the occurrence of the reforming reactions of CH_4 by both H_2O and CO_2 produced by the complete oxidation of the fuel. The subsequent

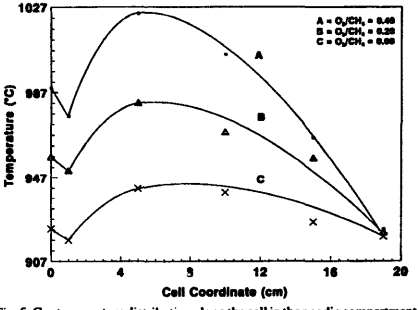

Fig. 5. Gas temperature distribution along the cell in the anodic compartment.

increase in temperature, which reaches a maximum at about 1/3 of the stack length, is due to the electrochemical oxidation of H_2 and CO; afterwards, the observed decrease is due to the dilution effect of the reaction products and to the heat exchange with the cathode air inlet. A preliminary modelling of the temperature and products distribution along the axis [11] proved to explain satisfactorily the above results.

Fig. 5 shows that, as the O_2/CH_4 ratio decreases, the temperature profile broadens progressively along the cell length. The region close to the fuel inlet is characterized by a temperature decrease due to the minor contribution of the deep oxidation. Accordingly, the lower amount of reaction products determines a lower temperature gradient in the endothermic reforming step following the deep oxidation. Subsequently, the electrochemical reaction products are partially involved as reactants in the reforming of the unreacted methane; thus, the simultaneous occurrence of endothermic reforming and exothermic electrochemical reactions results in a more homogeneous distribution of temperature along the cell length.

Further analysis of the present data can be accomplished by plotting the attained maximum power values versus the

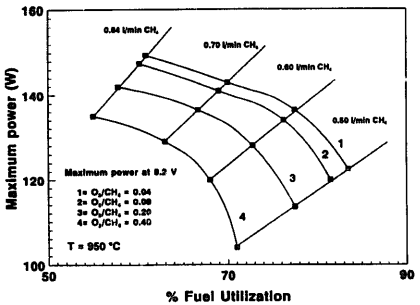

Fig. 6. Relationship between the fuel utilization and the maximum power attained at different O_2/CH_4 ratios at 950 °C.

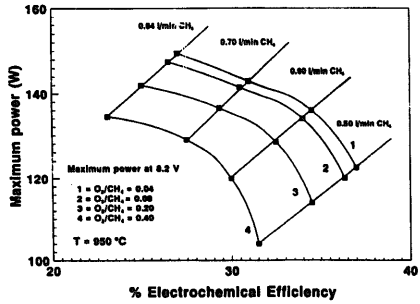

Fig. 7. Relationship between the electrochemical efficiency and the maximum power attained at different O_2/CH_4 ratios at 950 °C.

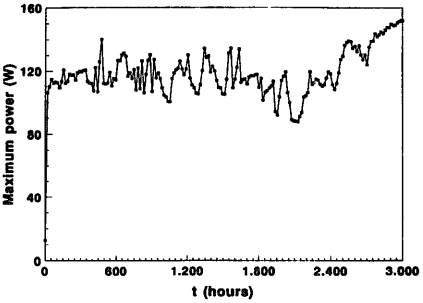

Fig. 8. Variation of the power attained during the 3000 h endurance test.

calculated fuel utilization and electrochemical efficiency data, presented in Figs. 6 and 7, respectively. Now, some considerations related to different possible options in the management of stack operations can be made. Low fuel utilizations appear to lead to high power values, in a large O_2/CH_4 interval (ranging from 0.04 to 0.4); thus, a fuel recycle option is to be taken into consideration in those cases where the attainment of large power levels is privileged. On the other hand, a nearly complete oxidation of the fuel will bring to sensibly lower overall performance. Parallel considerations clearly hold if the electrochemical efficiency parameter is taken into account; high power values can be achieved only under working conditions which allow the attainment of efficiency values not higher than 30%, also depending upon the anode feed composition (Fig. 7).

Fig. 8 shows the performance attained during a 3000 h endurance test which started at an air/CH_4 ratio 0.5, and was lowered to 0.27 during the last 600 h. A substantial steady response was observed during the whole test. The better performance observed during the last period appears to account for the already observed capability of the catalyst to withstand even very low O_2/CH_4 ratios, whose beneficial influence might be reconductable to a 'light-off' of the peripheral surface of the anode and no formation of carbon, at variance of the internal reforming.

5. Conclusions

The present results, although preliminary, appear to account for the feasibility of the CH_4 partial oxidation reaction as a promising option for natural gas-fuelled SOFC. This process allows to sustain autothermal operation of the fuel cell stack due to the exothermic character of the reaction. Further beneficial effects are represented by a fast start-up procedure and lower poisoning of the catalyst by carbon formation, with respect to internal reforming, due to the oxidative nature of the reaction.

However, the obtained results clearly indicate the need to develop a cost-effective catalyst (without noble metal) able

to withstand low O_2/CH_4 ratios in order to maintain high electrochemical efficiencies. Furthemore, the homogeneous temperature distribution along the tubular fuel cell unit avoids the occurrence of thermal stresses which likely represent the most critical issue for the development of SOFC.

References

[1] V. Antonucci, Advanced Solid Oxide Fuel Cells, *Proc. 6th IEA Workshop*, 1994, pp. 301–305.

[2] V. Antonucci, *Proc. 1st European Solid Oxide Fuel Cells Forum*, Vol. 1, 1994, pp. 183–195.

[3] V. Antonucci, G. Rocchini, P.L. Antonucci and N. Giordano, *Proc. 1994 Fuel Cells Seminar*, 1994, pp. 384–387.

[4] A.T. Ashcroft, A.K. Cheetham, J.S. Foord, M.L.H. Green, C.P. Grey, A.J. Mureel and P.D.F. Vernon, *Nature, 344* (1990) 319.

[5] P.D.F. Vernon, M.L.H. Green, A.K. Cheetham and A.T. Ashcroft, *Catal. Lett., 6* (1990) 181.

[6] J.S.J. Hargreaves, G.J. Hutchings and R.W. Joyner, *Nature, 348* (1990) 428.

[7] V. Antonucci, Design and construction of a 150 W SOFC station, *Rep. ENEL–CRTN, No 10–92*, 1992.

[8] D.W. Mckee, *Carbon, 23* (6) (1985).

[9] K. Otsuka, T. Ushiyama and I. Yamanaka, *Chem. Lett.*, (1993) 1517.

[10] D. Dissanajake, M. Rosynek, K. Kharas and J. Lunsford, *J. Catal., 132* (1991) 117.

[11] V. Antonucci, N. Giordano, P.L. Antonucci, E. Arato, P. Costamagna, G. Rocchini and A. Demit., *Proc. 4th Int. Congr. SOFC, Yokohama, Japan, 18–23 June 1995*, pp. 820–828.